AIP Journal of Applied Physics

Evaluating free vs bound oxygen on ignition of nano-aluminum based energetics leads to a critical reaction rate criterion

Wenbo Zhou, Jeffery B. DeLisio, Xizheng Wang, Garth C. Egan, and Michael R. Zachariah

Citation: Journal of Applied Physics **118**, 114303 (2015); doi: 10.1063/1.4930889
View online: http://dx.doi.org/10.1063/1.4930889
View Table of Contents: http://scitation.aip.org/content/aip/journal/jap/118/11?ver=pdfcov
Published by the AIP Publishing

Articles you may be interested in

Investigating the trade-offs of microwave susceptors in energetic composites: Microwave heating versus combustion performance
J. Appl. Phys. **115**, 104106 (2014); 10.1063/1.4868337

Pre-ignition laser ablation of nanocomposite energetic materials
J. Appl. Phys. **113**, 213107 (2013); 10.1063/1.4808458

Impact ignition of aluminum-teflon based energetic materials impregnated with nano-structured carbon additives
J. Appl. Phys. **112**, 024902 (2012); 10.1063/1.4737118

Transient ion ejection during nanocomposite thermite reactions
J. Appl. Phys. **106**, 083306 (2009); 10.1063/1.3225907

Nano-Aluminum Reaction with Nitrogen in the Burn Front of Oxygen-Free Energetic Materials
AIP Conf. Proc. **845**, 1022 (2006); 10.1063/1.2263496

HIDEN ANALYTICAL
Instruments for Advanced Science


Gas Analysis
- dynamic measurement of reaction gas streams
- catalysis and thermal analysis
- molecular beam studies
- dissolved species probes
- fermentation, environmental and ecological studies


Surface Science
- UHV TPD
- SIMS
- end point detection in ion beam etch
- elemental imaging - surface mapping


Plasma Diagnostics
- plasma source characterization etch and deposition process reaction
- kinetic studies
- analysis of neutral and radical species


Vacuum Analysis
- partial pressure measurement and control of process gases
- reactive sputter process control
- vacuum diagnostics
- vacuum coating process monitoring

Contact Hiden Analytical for further details:
W www.HidenAnalytical.com
E info@hiden.co.uk
CLICK TO VIEW our product catalogue

[This article is copyrighted as indicated in the article. Reuse of AIP content is subject to the terms at: http://scitation.aip.org/termsconditions. Downloaded to] IP: 128.8.176.93 On: Mon, 21 Sep 2015 14:12:05

Evaluating free vs bound oxygen on ignition of nano-aluminum based energetics leads to a critical reaction rate criterion

Wenbo Zhou, Jeffery B. DeLisio, Xizheng Wang, Garth C. Egan, and Michael R. Zachariah[a)]
Department of Chemical and Biomolecular Engineering, and Department of Chemistry and Biochemistry, University of Maryland, College Park, Maryland 20742, USA

(Received 23 June 2015; accepted 1 September 2015; published online 17 September 2015)

This study investigates the ignition of nano-aluminum (n-Al) and n-Al based energetic materials (nanothermites) at varying O_2 pressures (1–18 atm), aiming to differentiate the effects of free and bound oxygen on ignition and to assess if it is possible to identify a critical reaction condition for ignition independent of oxygen source. Ignition experiments were conducted by rapidly heating the samples on a fine Pt wire at a heating rate of $\sim 10^5$ °C s^{-1} to determine the ignition time and temperature. The ignition temperature of n-Al was found to reduce as the O_2 pressure increased, whereas the ignition temperatures of nanothermites (n-Al/Fe_2O_3, n-Al/Bi_2O_3, n-Al/K_2SO_4, and n-Al/$K_2S_2O_8$) had different sensitivities to O_2 pressure depending on the formulations. A phenomenological kinetic/transport model was evaluated to correlate the concentrations of oxygen both in condensed and gaseous phases, with the initiation rate of Al-O at ignition temperature. We found that a constant critical reaction rate (5×10^{-2} mol m^{-2} s^{-1}) for ignition exists which is independent to ignition temperature, heating rate, and free vs bound oxygen. Since for both the thermite and the free O_2 reaction the critical reaction rate for ignition is the same, the various ignition temperatures are simply reflecting the conditions when the critical reaction rate for thermal runaway is achieved.
© *2015 AIP Publishing LLC*. [http://dx.doi.org/10.1063/1.4930889]

I. INTRODUCTION

Recent advances in large-scale manufacturing and processing of nanoparticles have motivated research on energetic materials with nanoscale features and structures.[1–3] Nano-aluminum (n-Al), due to its high energy density and superior reactivity, is one of the most widely studied nanomaterials for pyrotechnics, propellants, and explosives applications.[4,5] A variety of powdered n-Al explosives and aluminized nanocomposites (nanothermites) that contain oxidizers are being evaluated based on their rate and intensity of energy release,[1–3] as well as their sensitivity and stability.[6,7] Compared to self-sustaining steady state combustion, reaction initiation (ignition) is difficult to study and control due to its very fast transient nature and its sensitivity to many parameters such as heating rate,[8,9] particle size,[10,11] and assembly[12,13] (influencing the contact area between fuel and oxidizer). For n-Al, ignition is further complicated by the thin (~2–5 nm) native oxide shell, alumina (Al_2O_3) that acts as a passivation layer at low temperatures.[14,15]

In order for ignition to occur, a threshold must be surpassed where the mutual transfer of Al and O across the Al_2O_3 shell is rapid enough to induce a sufficiently higher energy release rate relative to energy loss to the surroundings. It is expected that oxygen anions and aluminum cations migrate radially inward and outward, respectively, by the concentration gradients.[16] In addition, the outward transport of Al cations is primarily driven by a built-in electrical field across the alumina shell, as described by the Cabrera-Mott theory,[17,18] as well as by the pressure-driven outward convection due to the volumetric expansion of Al core during heating.[19,20] Given these two additional mechanisms, and that the Al cations are smaller than the oxygen anions,[16] the Al flux outwards should exceed that of oxygen inwards. This diffusion bias is prevailingly evidenced by several reports showing that hollow structures are formed during the oxidation of n-Al particles.[21–23] Therefore, the reaction interface is expected to be at the outer surface of the aluminum enriched alumina shell.[16,21]

Ignition of n-Al in gaseous oxidizers and of aluminum-fueled nanothermites relies on the same fundamental global reaction between Al and O. The distinction is that for nanothermites, the reactive oxygen that participates in the ignition event comes from oxygen bound in the oxygen lattice sites of the solid oxidizers. Based on the availability of free gaseous oxygen in the ignition event, the ignition mechanisms can be divided into two categories: (1) the condensed phase Al-O reaction and (2) the Al-O_2(g) heterogeneous reaction. For many Al/metal oxide formulations (e.g., Al/Bi_2O_3[24]), O_2 is released from oxidizers at a higher temperature than the corresponding ignition temperature, indicating that ignition is mainly triggered by the condensed phase reaction between Al and bound oxygen. In some other cases (e.g., Al/CuO[25]), oxygen release is prior too, or synchronized with ignition, suggesting that the predominant reactive oxygen that participates in the initiation reaction could be gaseous O_2. A recent study has investigated ignition temperatures of multiple oxysalt based thermites in various gaseous environments.[26] The results show that some reactive oxysalts, such as potassium periodate (KIO_4)[27] and potassium persulfate ($K_2S_2O_8$),[28] are more easily decomposed than traditional metal oxides, thus exhibiting very low O_2 release temperatures and ignition temperatures. In this case, it is believed that free gaseous O_2

[a)]Author to whom correspondence should be addressed. Electronic mail: mrz@umd.edu. Tel.: 301-405-4311. FAX: 301-314-9477.

 © 2015 AIP Publishing LLC

[This article is copyrighted as indicated in the article. Reuse of AIP content is subject to the terms at: http://scitation.aip.org/termsconditions. Downloaded to] IP: 128.8.176.93 On: Mon, 21 Sep 2015 14:12:05

plays the predominant role in triggering the ignition event.[26–28] Due to the reactive sintering of fuel and oxidizer at the initiation stage for many thermite formulations as observed from post-reaction products analysis[29,30] and *in situ* fast-heating electron microscopy,[29,31,32] the two aforementioned ignition mechanisms may be actually coincident in a single ignition event. While many studies have supported these two main ignition mechanisms, they fail to explain when these different mechanisms exist, and under what conditions they prevail.[28,33]

Previous studies have presented a muddled vision of the criteria that control the ignition of n-Al based energetic materials. The melting point of Al, or the decomposition temperature of oxidizer, has been presumed as the criterion for ignition.[34,35] However, some experimental results have also revealed that there is no correlation between these characteristic temperatures and ignition temperature.[36] These results suggest that the ignition phenomenon is not merely driven thermodynamically but is also driven kinetically. Previous kinetic models have been proposed for the oxidation of n-Al in which power-law functions were adopted to describe the oxidation rate of Al.[37–39] Since these functions were developed to describe oxidation kinetics when a significant conversion from Al to Al_2O_3 had occurred, they are inappropriate for ignition kinetics, which feature a very small conversion ratio. Alternatively, zero-order Arrhenius models involving no concentration of reactants,[40,41] and 1st order models which include oxygen concentration as a parameter, have been employed.[42] However, given that the concentration of Al at the reaction interface may also change with temperature,[14,19,22,34–36,43–45] an improved model containing both concentrations of Al and O needs to be evaluated. In addition, some consideration should be given which will shed light on the aspect of metal ignition when the source is free O_2 vs bound oxygen.

In this work, the ignition of n-Al based energetic materials was analyzed to explore the role of bound vs free oxygen, and to assess if it is possible to identify a critical reaction condition for ignition independent of oxygen source. For these studies, we evaluate the ignition of n-Al and four aluminum based nanothermites (n-Al/Fe_2O_3, n-Al/Bi_2O_3, n-Al/K_2SO_4, and n-Al/$K_2S_2O_8$) in O_2. What distinguishes this particular work is that we simultaneously varied the O_2 concentration as a control variable through the initial pressure (1–18 atm). The experimental results were used in conjunction with a phenomenological kinetic/transport model to determine a critical condition for ignition and a global activation energy. When combined with the experimental results, the model enables us to distinguish the role of free vs bound oxygen on ignition. The result shows that the critical reaction condition for ignition is independent of oxygen source and heating rate.

II. EXPERIMENTAL SECTION

A. Materials

n-Al particles (~50 nm) were obtained from Argonide Corporation. Bismuth oxide (Bi_2O_3) and iron oxide nanoparticles (Fe_2O_3) (~50 nm) were obtained from Sigma-Aldrich. Microscale potassium persulfate ($K_2S_2O_8$) and potassium sulfate (K_2SO_4) powders were purchased from Fluka and Sigma Aldrich, respectively. Nanoscale potassium persulfate ($K_2S_2O_8$) and potassium sulfate (K_2SO_4) were prepared by spray drying of the $K_2S_2O_8$ water solution (0.02 mol l^{-1}) at 150 °C, and the K_2SO_4 water solution (0.02 mol l^{-1}) at 180 °C, respectively.[26,28] Nanothermites were prepared by sonicating the n-Al and nanoscale oxidizers stoichiometrically in hexane for 30 min, followed by stirring overnight and desiccation in vacuum.

B. Temperature jump (T-jump) ignition measurements

The ignition tests were conducted by coating the hexane suspension of n-Al or aluminum-fueled nanothermites evenly onto a (76 μm diameter × 10 mm long) platinum (Pt) wire. The particle layer was found to have a length of ~8 mm and a thickness of 25 μm. In the case of ignition of n-Al, the mass of n-Al was estimated to be ~30 μg, assuming that the sample pack density on wire is ~20%.[25] In the case of ignition of nanothermites, we controlled the same coating volume of samples on wire as that for n-Al, and the masses were around 30 μg–75 μg depending on the formulations. After drying in air, the wire was resistively heated to ~1200 °C within 3 ms (~4×10^5 °C s^{-1}) by a tunable voltage pulse generated by a home-built power source (Fig. S1[46]). For any given voltage, the current passing through the wire was measured using a current probe (AM503, Tektronix). The transient voltage and current were simultaneously recorded into an oscilloscope (WR 606Zi, Teledyne-LeCroy). The transient temperature on the wire during the pulse time was measured according to the standard electrical resistance/temperature relationship for Pt (Callendar-Van Dusen equation[47]). The ignition time was determined using a high speed camera (Vision Research Phantom v12.0) (Fig. S1[46]) and identified as the onset time of an appreciable emission of light above the background signal from the wire. A new T-jump Pt wire was used for each experiment. Our previous analysis shows that for a particle layer up to ~30 μm in thickness, the difference in temperatures of particle layer and basement wire is not discernible.[25] This indicates that the temperature of nanopowders approximately matches the temperature on the wire prior to ignition.

To control the ignition of n-Al in different O_2 pressures, the T-jump probe was placed in a chamber that enabled ignition conditions to be varied from 10^{-10} atm up to 18 atm (Fig. S1[46]). To control the ignition of n-Al at different heating rates, n-Al was heated to the same peak temperature of ~1200 °C but within different pulse times (2 ms, 4 ms, 8 ms, and 16 ms). A thinner Pt wire (radius = 12.7 μm) was also used in the ignition test of n-Al in O_2, to evaluate if the results were dependent on wire diameter. The mass loaded on the thinner wire was kept constant as ~20 μg.

[This article is copyrighted as indicated in the article. Reuse of AIP content is subject to the terms at: http://scitation.aip.org/termsconditions. Downloaded to] IP: 128.8.176.93 On: Mon, 21 Sep 2015 14:12:05

III. RESULTS AND DISCUSSION

A. Ignition of n-Al in free oxygen

In order to evaluate the role of free O_2, the chamber was filled with the pure gas at pressures ranging from 10^{-10} atm to 18 atm. Fig. 1 shows that the ignition temperature decays with increasing O_2 pressure, and drops below the melting point of bulk Al at >7.4 atm. As the O_2 pressure further increases to over 15 atm, the ignition temperature asymptotically approaches a value of ~620 °C. This threshold implies that ignition at this point is limited by the mobility of Al migrating outwards, so that below a critical temperature, the surface concentration of Al is too low to support the ignition event. Considering that a smaller particle size is able to depress the ignition temperature of bulk Al,[36] this critical temperature is probably correlated with the melting of n-Al. This strong dependence on O_2 pressure for ignition temperature represents a thermodynamic state (i.e., temperature) for rapid kinetics sufficient for run-away reaction.

B. Ignition of n-Al based thermites (i.e., bound oxygen)

In the previous example, O_2 was free and its concentration was systematically varied by changing the pressure. Next, bound oxygen was investigated through the ignition of four n-Al based thermites (n-Al/Fe_2O_3, n-Al/Bi_2O_3, n-Al/K_2SO_4, and n-Al/$K_2S_2O_8$). Fig. 2 shows that these nanothermites have a wide range of ignition temperatures in vacuum, with the highest ignition temperature for n-Al/Fe_2O_3 at 825 °C, and the lowest for n-Al/Bi_2O_3 at 590 °C. Since a low pressure environment will promote rapid extraction of any gaseous O_2 generated by the oxidizer away from the thermite mixture on the wire, the initiation reaction for these nanothermites in vacuum (~10^{-10} atm) should be predominantly controlled by the condensed phase reaction. Given that the ignition temperatures follow: n-Al/Fe_2O_3 > n-Al/K_2SO_4 ≈ n-Al/$K_2S_2O_8$ > n-Al/Bi_2O_3, and there is only a small difference in the oxygen densities of the four oxidizers, the different ignition temperatures in vacuum are more likely to be correlated to different activation energies of these four condensed phase Al-O reactions.

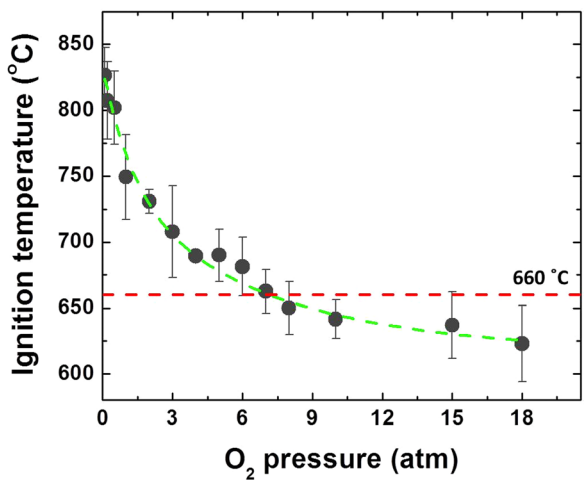

FIG. 1. Ignition temperature of n-Al vs external oxygen gas pressure. Each data point represents the average of at least three measurements. The error bars of ~10% are mainly from our temperature measurement which has a degree of inaccuracy of ±25 °C.

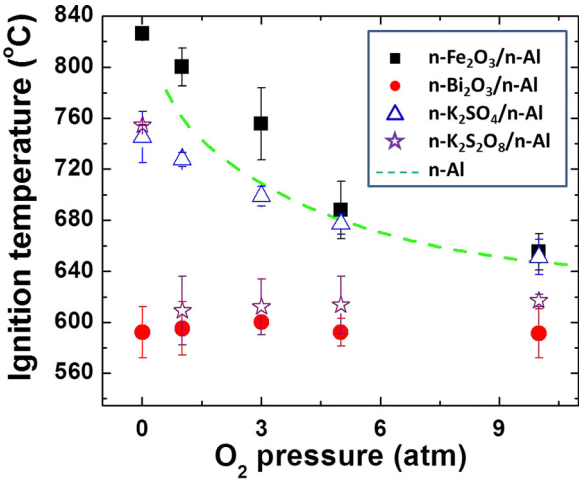

FIG. 2. Ignition temperatures for four different n-Al based thermites (n-Al/Fe_2O_3, n-Al/Bi_2O_3, n-Al/K_2SO_4, and n-Al/$K_2S_2O_8$) as a function of external oxygen pressure. Each data point represents an average of at least two measurements. The decaying dashed line represents a fit for pure n-Al from the data in Fig. 1.

Increasing the O_2 pressure resulted in a variety of mainly decreasing trends that were dependent on the thermite system. The decaying dashed line represents a fit for pure n-Al from the data in Fig. 1. For the case of n-Al/Bi_2O_3, which already possesses a low ignition temperature, increasing the O_2 concentration has no discernible effect. This confirms previous work[33] that the initiation of the n-Al/Bi_2O_3 is controlled exclusively by a condensed phase reaction, with ignition occurring much earlier than the decomposition temperature of Bi_2O_3 (~1300 °C). This behavior has been explained by the fact that Bi_2O_3 has one of the highest known oxygen ion conductivities among typically used oxidizers,[48] which would greatly enhance condensed phase transport of oxygen.

The opposite extreme to the Bi_2O_3 containing system would be one where gas phase O_2 is released from the oxidizer at a lower temperature than ignition.[27] One such system is n-Al/$K_2S_2O_8$, which shows a significant reduction of ignition temperature in O_2 (610 °C) when compared to that in vacuum (755 °C). If condensed phase reactions were important, then we should expect no decrease in ignition temperature between vacuum and 1 atm. However, the fact that increasing pressure of O_2 does not change the ignition temperature implies that O_2 release from n-Al/$K_2S_2O_8$ is controlling. Furthermore, the fact that this reaction has a lower ignition temperature than the neat n-Al in O_2, as represented by the decaying dashed line (Fig. 2), is consistent with the fact that the oxygen concentration in solid oxidizers (7×10^4 mol m^{-3}) is more than 2 orders of magnitude higher than that in gas (1–100 mol m^{-3} when the O_2 pressure changes from 0.1 atm to 18 atm (Fig. 1)). Thus, in the case of $K_2S_2O_8$, the bound oxygen is released at much higher concentration than the local O_2 pressures tested in this experiment.[27,28]

[This article is copyrighted as indicated in the article. Reuse of AIP content is subject to the terms at: http://scitation.aip.org/termsconditions. Downloaded to] IP: 128.8.176.93 On: Mon, 21 Sep 2015 14:12:05

For the other two investigated nano-thermite formulations, the ignition temperatures decrease as the O_2 pressure increases (Fig. 2). At O_2 pressures below 5 atm, the ignition temperatures of n-Al/Fe_2O_3 are higher than the corresponding ignition temperatures of n-Al, while the ignition temperatures of n-Al/K_2SO_4 are in contrast lower (Fig. 2). We have seen in Fig. 2 that the ignition points of n-Al/Fe_2O_3 and n-Al/K_2SO_4 in vacuum are above and below the dashed line, respectively, indicating that the reaction rate between Al and bound oxygen from Fe_2O_3 is slower than that between Al and free O_2, while the reaction rate between Al and bound oxygen from K_2SO_4 is higher. If we consider the overall initiation reaction for these two nanothermites are comprised of two competitive reactions (Al reacting with gaseous oxygen and condensed phase oxygen), since the reaction rates follows: Al-O (from K_2SO_4) > Al-O_2 (g) > Al-O (from Fe_2O_3), one would expect to see that ignition temperatures follows: n-Al/Fe_2O_3 > n-Al > n-Al/K_2SO_4, consistent with our experimental results in the O_2 pressure range of 1–5 atm (Fig. 2). At O_2 pressures above 5 atm, their ignition temperatures asymptotically approach the corresponding ignition temperature of n-Al (Fig. 2). This indicates that once more gaseous oxygen is added, n-Al in the formulation initiates predominantly by a relatively more reactive Al-O_2 (g) mechanism, and the oxidizers gradually become dead weight in the system until after ignition.

C. Thermal transfer analysis and criterion for n-Al at ignition

The ignition results of n-Al and n-Al based nanothermites have suggested that ignition temperature is controlled by the local concentration of oxygen, either in the condensed phase as in the case of Bi_2O_3 or alternatively as an effective local O_2 concentration as in the case of $K_2S_2O_8$. A higher oxygen concentration (or lower activation energy) would lead to a larger reaction rate between Al and O, which as a result induces more heat generation at a given temperature. To evaluate these results more thoroughly, we will develop a relationship between a global reaction rate at the point of ignition (R_c), and the ignition temperature. We assume that n-Al has a radius r of ~25 nm and an alumina shell thickness d of ~4 nm, which is roughly consistent with the n-Al employed in the experiments. Since only one size of n-Al was used in this study, the effect of contact area between Al and O was not considered. The energy balance for the n-Al coated Pt wire is as follows (also see Fig. S2(a)[46]):

$$\dot{q}_a = \dot{q}_r + \dot{q}_{e,loss} + \dot{q}_{gain} + \dot{q}_{c,loss} + \dot{q}_{rad,loss} + \dot{q}_{r,evap}, \quad (1)$$

where $\dot{q}_a$ is the net accumulated energy of the n-Al coated Pt wire, $\dot{q}_r$ is the generated energy from the Al-O reaction, $\dot{q}_{e,loss}$ is the energy loss from Al evaporation, $\dot{q}_{gain}$ is the energy gain from the resistive heating of the wire, $\dot{q}_{c,loss}$ is the conducted energy loss to the environment (mainly the electrodes that hold the wire), $\dot{q}_{rad,loss}$ is the heat loss by radiation, and $\dot{q}_{r,evap}$ is the heat generated from the reaction of O_2 and gaseous Al evaporated from the particle surface.

At the peak temperatures around the point of ignition, Al evaporation and thermal irradiation are not significant; the heat accumulation is mainly dominated by the resistive heating of the wire ($\dot{q}_{gain}$), the energy gain by reaction ($\dot{q}_r$), and the heat loss to the environment ($\dot{q}_{c,loss}$). Thus, Eq. (1) at peak temperatures around ignition point can be simplified as

$$\dot{q}_a = \dot{q}_{gain} + \dot{q}_r + \dot{q}_{c,loss}. \quad (2)$$

In Eq. (2), $\dot{q}_a$ and $\dot{q}_r$ can be expressed as follows:

$$\dot{q}_a = (n_{\mathrm{Al}} Cp_{\mathrm{Al}} + n_{\mathrm{Pt}} Cp_{\mathrm{Pt}}) \frac{dT}{dt}, \quad (3)$$

$$\dot{q}_r = 4\pi r^2 R \Delta H_r N_{n-\mathrm{Al}}, \quad (4)$$

where n_{Al} and n_{Pt} are the molar amounts of Al and Pt, Cp_{Al} and Cp_{Pt} are the heat capacities of Al and Pt (Cp_{Pt} = 25.86 J mol^{-1} °C^{-1}),[49,50] ΔH_r is the heat of reaction per mole of Al (= 837.5 kJ mol^{-1}),[22] $N_{n\text{-Al}}$ is the number of n-Al particles loaded on the wire, and R is the reaction rate. Since $n_{Al} \ll n_{Pt}$ in our system, Eq. (3) can be simplified as $\dot{q}_a = n_{\mathrm{Pt}} Cp_{\mathrm{Pt}} dT/dt$. According to the dimension of the Pt wire (length = 1 cm, radius = 38.1 μm), as well as the density of Pt at the room temperature (= 21.45 g cm^{-3}), the molar amount of Pt (n_{Pt}) is calculated to be 5.1×10^{-6} mol. Considering that the mass loading on the wire is ~30 μg in the case of ignition of n-Al in O_2, $N_{n\text{-Al}}$ is calculated to be 1.9×10^{11}. For the ignition of nanothermites, $N_{n\text{-Al}}$ are distinct for different formations based on different total mass loading. In detail, $N_{n\text{-Al}}$ for n-Al/Fe_2O_3, n-Al/K_2SO_4, n-Al/$K_2S_2O_8$, and n-Al/Bi_2O_3 are 0.76×10^{11}, 0.32×10^{11}, 0.38×10^{11}, and 0.48×10^{11}, respectively.

Using our T-Jump heating experiment, the temporal temperature history for n-Al particles, which is consistent with the temporal temperature history for the carrier Pt wire, was recorded during the 3 ms pulse time. For a 5 atm external pressure of O_2, a typical temperature-time curve for n-Al in the neighborhood of ignition temperature is shown in Fig. 3. The experimental temperature curve has a width of ~50 °C (as

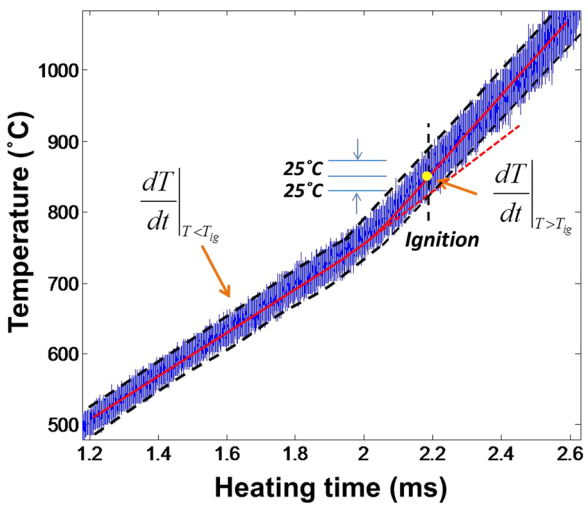

FIG. 3. Experimental temporal temperature profile on n-Al particles. A fitted solid curve (red) was centered along the raw curve (blue). The width of our raw curve is 50 °C (as shown in between two dashed curves along the raw curve), demonstrating that the accuracy of the temperature measurement is ±25 °C. The temperature gradients for n-Al before and after ignition, as well as the ignition point, are labeled.

[This article is copyrighted as indicated in the article. Reuse of AIP content is subject to the terms at: http://scitation.aip.org/termsconditions. Downloaded to] IP: 128.8.176.93 On: Mon, 21 Sep 2015 14:12:05

shown by the two dashed curves), demonstrating that the precision of the temperature measurement is ±25 °C. It can be seen that the slope of temperature-time curve ($dT/dt|_{T<T_{ig}}$) for n-Al is close to constant, and equivalent to the slope of temperature-time curve on the bare wire ($dT/dt|_{wire}$) (without deposition of n-Al) below the ignition point (Fig. 3). This is consistent with the fact that prior to ignition, the heat accumulation is exclusively from the resistive heating of the wire ($\dot{q}_{gain}$) subtracted by the heat loss to the environment ($\dot{q}_{c,loss}$). So, Eq. (2) prior to ignition can be expressed as

$$\dot{q}_a|_{T<T_{ig}} = \dot{q}_{gain} + \dot{q}_{c,loss}. \tag{5}$$

At the point of ignition, a rapid excursion in the wire temperature (Fig. 3) occurs that leads to a higher slope of temperature-time curve ($dT/dt|_{T>T_{ig}}$). This result is indicative that the heat generated by reaction ($\dot{q}_r$) becomes significant. From the temperature-time curve for the bare Pt wire, we also know $\dot{q}_{gain}$ and $\dot{q}_{c.loss}$ are constants in the neighborhood of ignition point. In this regard, the energy balance at the point of ignition is

$$\dot{q}_a|_{T>T_{ig}} = \dot{q}_{gain} + \dot{q}_r^{\bullet} + \dot{q}_{c,loss}. \tag{6}$$

By combing Eqs. (5) and (6), we find that the reaction rate, R_c, at the ignition temperature can be taken as a function of the temperature gradient difference as

$$R_c = \frac{n_{Pt} C p_{Pt}}{4\pi r^2 \Delta H_r N_{n-Al}} \left(\left.\frac{dT}{dt}\right|_{T>T_{ig}} - \left.\frac{dT}{dt}\right|_{T<T_{ig}} \right). \tag{7}$$

It should be noted that the ignition point we chose in Fig. 3 is not the inflection point of the curve. This is to account for the uncertainty in the temperature measurement which as can be seen in the figure is ~±25 °C. Ignition is defined as the point where the extrapolation of the ignition curve deviated by at least the uncertainty (25 °C). In regard to Eq. (7), the value of $dT/dt|_{T>T_{ig}}$ is defined as the slope at this point, which can be approximated by the average slope of fitted wire within the temperature range of ±50 °C of the ignition point. This definition of ignition point is different from that we utilized to measure the ignition temperatures of n-Al based energetic materials, which is determined by the onset of light emission from ignition.[24–27] However, since we found that these two defined ignition temperatures are usually very close (<50 °C), we will use the current definition of ignition temperature for the following energy balance analysis.

In Eq. (7), the number of n-Al loaded on wire is an estimated value based on our calculation from an ideal geometry of the nanoparticle coating. The actual measurement of the mass gravimetrically confirms that the deposit of n-Al is ~30 ± 10 μg, which gives an uncertainty of 50% to the R_c value.

Eq. (7) forms the basis of the following discussion to evaluating the ignition criteria.

D. Critical reaction rate of n-Al with free and bound oxygen

Ignition is nominally the point when the exothermicity of a reaction exceeds the energy dissipation rate, which we can define as the critical reaction rate R_c. The question at hand is that given the similarity between the overall chemistry there is the critical reaction rate independent of the source of oxygen. In terms of our model (Fig. 3), by keeping constant all other external conditions that may influence the energy balance, such as the deposited mass on wire, the value of R_c is exclusively dependent on the temperature gradient difference before and after ignition (Eq. (7)). Evaluation of Eq. (7) from the measured temperature profiles of ignition experiments in different O_2 pressures (Fig. 1) shows that the R_c for ignition is indeed a constant over a range of ignition temperatures, with an average value of 5×10^{-2} mol m^{-2} s^{-1} (Fig. 4(a)). This is further confirmed from another experiment using a thinner mass-loaded Pt wire (radius = 12.7 μm) which has a mass one ninth of that for the normal wire (radius = 38.1 μm). At 3 atm O_2 pressure, the difference of temperature slopes before and after ignition point increased by nine folds when compared to that for normal wire. According to Eq. (7), these changes in temperature slope difference and Pt content result in a R_c (6.7×10^{-2} mol m^{-2} s^{-1}) that is similar to those (5×10^{-2} mol m^{-2} s^{-1}) obtained from our standard wire diameter experiments (see the star point in Fig. 4(a)). These results indicate that the role of O_2 is to enable achieving the critical reaction condition at a lower temperature for an increased concentration of O_2.

We next explore if the critical reaction rate is dependent on the heating rate. The corresponding ignition experiments for pure n-Al were conducted at different initial heating rates in 3 atm O_2 by using different pulse times (2–16 ms).

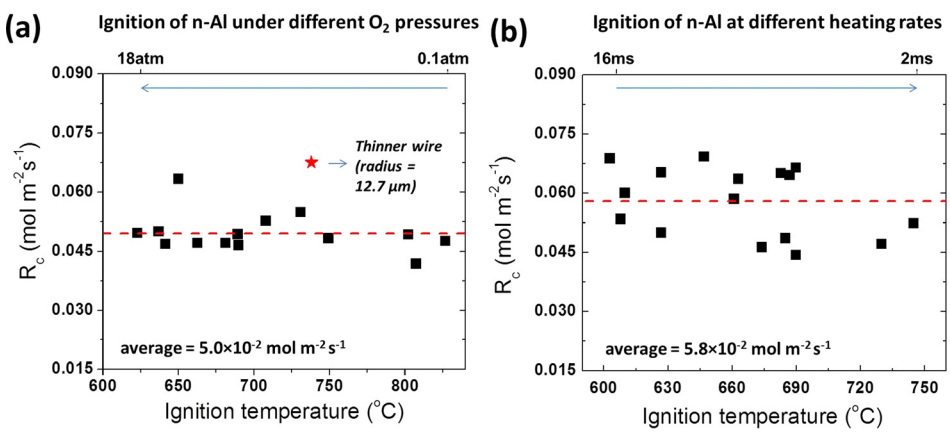

FIG. 4. Critical reaction rate (R_c) evaluated from Eq. (7) at ignition temperatures for n-Al under different O_2 pressures (0.1–18 atm) at a constant initial heating rate (~4×10^5 °C s^{-1}) (a), and under a constant O_2 pressure (3 atm) at different initial heating rates (~1×10^5–~6×10^5 °C s^{-1}) (b). The star point in (a) represents the R_c of n-Al on a thinner Pt wire (radius = 12.7 μm), corresponding to an ignition temperature of 738 °C and external O_2 pressure of 3 atm.

[This article is copyrighted as indicated in the article. Reuse of AIP content is subject to the terms at: http://scitation.aip.org/termsconditions. Downloaded to] IP: 128.8.176.93 On: Mon, 21 Sep 2015 14:12:05

Fig. 4(b) shows that over the range of heating rates from ~1 × 10^5 °C s^{-1} to ~6 × 10^5 °C s^{-1}, the ignition temperature of n-Al increases by 150 °C. However, the critical reaction rate remains constant at ~5.8 × 10^{-2} mol m^{-2} s^{-1}, which is similar to the value we obtained from ignition experiments when oxygen pressure was varied (Fig. 4(a)). The two experiments offer the same conclusion, namely, that there exists a critical reaction rate that determines the initiation of reaction between Al and oxygen.

The critical reaction rate of Al with bound oxygen in the nano-thermites was also evaluated from the data in Fig. 2. In vacuum, the unavailability of gas presumably ensures that all nanothermite ignition follows a condensed phase mechanism (Fig. 2). Similar to the aforementioned ignition of n-Al in O_2 (Fig. 1), the ignition reaction rate of each thermite formulation can be calculated according to Eq. (7) under the vacuum condition case. Since Eq. (7) is based on an energy balance that assumes nothing about where oxygen comes from, it is equally applicable to the measurement of the critical reaction rate for thermites. The R_c'*s* for the four thermite formulations were found to be similar (3.5 × 10^{-2}–5.9 × 10^{-2} mol m^{-2} s^{-1}, see Table I), which are also equivalent to the reaction rate of pure n-Al in O_2 (Fig. 4), and independent of ignition temperature. Thus, a critical reaction rate for ignition, if it exists, should have a characteristic that it be constant and invariant of other factors such as ignition temperature, heating rate, and oxygen source.

The key point, however, is to note that in both the thermite and the free O_2 reaction the critical reaction rate for ignition is the same, and the various ignition temperatures are simply reflecting the conditions when the critical reaction rate for thermal runaway is achieved.

It may seem, at first consideration, odd that both the free and bound oxygen case have essentially the same critical reaction rate. However, when one considers these global reactions, they are actually very similar in both the free and bound oxygen cases. First, it must be considered that the same fuel particles are used in every case, so while the given reaction rate is normalized by surface area, the result is the same for both cases. Thus, this critical reaction rate implies that, at ignition, the energy generation rate is the same for both free and bound oxygen systems. Second, the thermochemistry of the reaction of all the systems is quite similar, as it is dominated by the exothermic generation of Al_2O_3. If we consider a metric of the heat of reaction normalized by the heat capacity, which is a measure of how much the temperature of the energetic material will rise per unit of reaction, we find that all systems are within a factor of 2. Thus, the result that the critical reaction rates for thermal runaway for both the free and bound oxygen cases are similar is perhaps not so surprising.

TABLE I. Ignition temperatures in vacuum, interfacial concentrations of oxygen and aluminum at the ignition temperatures, the activation energies of the condensed phase Al-O reaction, as well as the condensed phase ignition reaction rates for n-Al/Fe_2O_3, n-Al/Bi_2O_3, n-Al/K_2SO_4, and n-Al/$K_2S_2O_8$.

Formulations	E_a^s (kJ/mol)	R_c' (mol/(m^2 s))
n-Al/Bi_2O_3	146[a]	4.1 × 10^{-2}
n-Al/K_2SO_4	167[a]	5.9 × 10^{-2}
n-Al/$K_2S_2O_8$	169[a]	4.9 × 10^{-2}
n-Al/Fe_2O_3	181[a]	3.5 × 10^{-2}
n-Al	134[b]	5.0 × 10^{-2}

[a]Activation energy of condensed phase reaction of Al and O(s).
[b]Activation energy of heterogeneous reaction of Al and O_2(g).

E. Arrhenius parameters (free and bound) at ignition

One key takeaway from our results is that the various ignition temperatures are simply reflecting the conditions when the critical reaction rate for thermal runaway is achieved. While this ignition criterion is able to generally determine when ignition initiates, it does not provide us details about why different formulations show different ignition temperatures. We next explicitly investigate several vital factors (oxygen concentrations, activation energy, etc.) that contribute to the global reaction rate, aiming to systematically understand the control of ignition. From the results in Figs. 1 and 2, we have seen the critical roles of oxygen concentration and activation energy in controlling ignition temperature, though we did not evaluate these parameters in a quantitative manner. On the other hand, as the other reactant at ignition, the concentration of Al at the reaction interface also contributes to the reaction rate. As the temperature increases, Al will become increasingly mobile and migrate through the oxide shell driven by pressure, concentration gradient, and built-in electric fields.[17–20] The prevailing evidence shows that aluminum flux outward exceeds that of oxygen inwards, thus indicating that the Al-O reaction occurs at the outer surface of the aluminum enriched alumina shell.[16,21] Given that both concentrations of Al and O change with temperature, we can explore the above ignition criterion further by explicitly evaluating a rate law for R_c, expressed as

$$R_c = k(C_{\mathrm{Al}}^s)^m (C_{\mathrm{O}})^n, \tag{8}$$

where

$$k = A \exp\left(-\frac{E_a}{\bar{R}T}\right). \tag{9}$$

Here, k is the reaction constant, C_{O} and C_{Al}^s are the concentrations of reactive oxygen and aluminum at the reaction interface, m and n are positive indices of C_{Al}^s and C_{O}, respectively, A is the pre-exponential factor, and E_a is the activation energy of the Al-O reaction. For the fast initiation of n-Al in O_2, both thermochemical calculations (using NASA CEA Code) and tests by T-jump time-of-flight mass spectrometry (TOF-MS) have demonstrated that the major intermediate product is Al_2O.[51] This implies that for the initial Al-O reaction, the production of Al_2O intermediates prevails. Therefore, the rate law is taken as $m = 1$, $n = 0.5$. If we further assume that the concentration of oxygen in the proximity of reaction interface is similar or at least scales with the external oxygen pressure ($C_{O2} = 0.5\ C_{\mathrm{O}}$), the kinetic equation is

[This article is copyrighted as indicated in the article. Reuse of AIP content is subject to the terms at: http://scitation.aip.org/termsconditions. Downloaded to] IP: 128.8.176.93 On: Mon, 21 Sep 2015 14:12:05

$$R_c = A\exp\left(-\frac{E_a}{\bar{R}T}\right)C_{\mathrm{Al}}^{s}(2C_{\mathrm{O2}})^{0.5}, \tag{10}$$

where $\bar{R}$ is the universal gas constant.

To evaluate the activation energy (E_a), we employ the Flynn–Wall–Ozawa isoconversion method[52,53] as

$$\ln\beta = const. - \frac{1.052E_a}{\bar{R}T}. \tag{11}$$

To do this, the ignition temperature of n-Al at 1 atm O_2 was evaluated at different heating rates (β) from 7.5 $\times 10^4$ °C s^{-1} to 6 $\times 10^5$ °C s^{-1}. The slope of the Arrhenius plot of heating rate vs ignition temperature shown in Fig. 5(a) yields an activation energy of 134 kJ mol^{-1}. Similar experiments at 3 atm O_2 yield a similar result of 137 kJ/mol (Fig. S4[46]), indicating that it is independent of O_2 concentration. It should be noted that the activation energy measured here is smaller than most of the activation energies of Al oxidation previously reported;[14] however, Jian *et al.*[54] reported a similar result showing that the decomposition of metal oxides at high heating rates ($\sim 10^5$ °C s^{-1}) has lower activation energies than the values found at low heating rates. They attributed the decrease in activation energy to the mass-transfer constraints at higher heating rates.

In order to evaluate the pre-exponential factor A, it is necessary to estimate the surface aluminum concentration, C_{Al}^{s}, which we do by a simple transport analysis. In principle, the outward transport rate of Al should be equivalent to the sum of the reaction rate of Al with O at the particle surface, the evaporation rate of Al from the particle, as well as the accumulation rate of Al at the surface (Fig. S2(b)[46]). Since our focus is on ignition where the reaction of Al and O becomes significant, the outwardly diffused Al is presumably consumed rapidly suggesting no accumulation of Al on the reaction interface. Therefore, the mass balance at the ignition temperature can be expressed as follows:

$$j_{\mathrm{Al}}^{evap} + R_c = j_{\mathrm{Al}}^{E} + j_{\mathrm{Al}}^{P}, \tag{12}$$

where j_{Al}^{evap} is the evaporation flux of Al escaped from the particle surface, j_{Al}^{E} is the diffusion fluxes of Al through the alumina shell driven by the built-in electrical field.[17–20] j_{Al}^{P} is the convection flux of Al through the alumina shell driven by the internal pressure.[17–20] Since the Al flux due to the concentration gradient was reported to be smaller than the other flux terms,[19] we will neglect it in the following analysis. The detailed expressions of these flux terms can be found in the supplementary material (Eqs. (S1)–(S4)).[46]

Eq. (12) can be further simplified after comparing the dimensions of the three flux terms it contains. In terms of our results on ignition of n-Al in different O_2 pressures (Fig. 1), j_{Al}^{E} was ~1 order and ~6 orders of magnitude larger than j_{Al}^{P} and j_{Al}^{evap}, respectively (Fig. S5[46]), within the ignition temperature range in Fig. 1. Therefore, Eq. (12) was simplified as $R_c = j_{\mathrm{Al}}^{E}$, and can be extended by plugging in the expression of j_{Al}^{E}, which is the electric field driven oxidation (see Eq. (S3) in the supplementary material[46]),

$$C_{\mathrm{Al}}^{S} = \frac{\bar{R}Td}{zFD\Delta\phi}R_c, \tag{13}$$

where D is the diffusion coefficient of Al ($= 4.9\times10^{-11}\exp(-4240/T)$ m^2 s^{-1}),[22] $\Delta\Phi$ is the Mott potential ($= -1.6$ V for n-Al),[17,18] z is the valency of Al ions ($= 3$), F is the molar charge of Al ions ($= 96485$ C mol^{-1}), C_{Al}^{s} is the surface concentration of Al on the outer alumina shell, and d is the alumina shell thickness ($= 4$ nm). Given that R_c at different O_2 pressures was already measured, the above C_{Al}^{s} can be estimated using likely $\Delta\Phi$ and D, obtained from other studies. The detailed interpretation of these approximations can be found in the supplementary material.[46]

Given that the values of E_a, C_{Al}^{s}, and C_{O_2} are known (Figs. 5(a) and S3[46]), we can calculate the pre-exponential factor (A). This value is shown in Fig. 5(b) as a function of ignition temperature and appears to be a constant with the average value of 2 $\times 10^5$ $m^{2.5}$ $mol^{-0.5}$ s^{-1} (Fig. 5(b)).

We now turn our attention to ignition in the presence of bound-oxygen. If we consider the ignition of nanothermites that undergo a condensed phase reaction as the reaction between the diffusing Al and bound oxygen from oxidizers, we can define the reaction rate in a similar manner,

$$R_c{}' = A'\exp\left(-\frac{E_a^s}{\bar{R}T}\right)C_{\mathrm{Al}}^{s}C_{\mathrm{O}}^{s\,0.5}. \tag{14}$$

Here, $R_c{}'$ is the condensed phase critical reaction rate, A' is the pre-exponential factor for the condensed phase reaction, E_a^s is the activation energy of condensed phase Al-O reaction, and C_{O}^{s} is the interfacial concentration of reactive oxygen in the condensed phase. For a given thermite formulation, both reaction mechanisms in Eqs. (10) and (14) may exist. If we

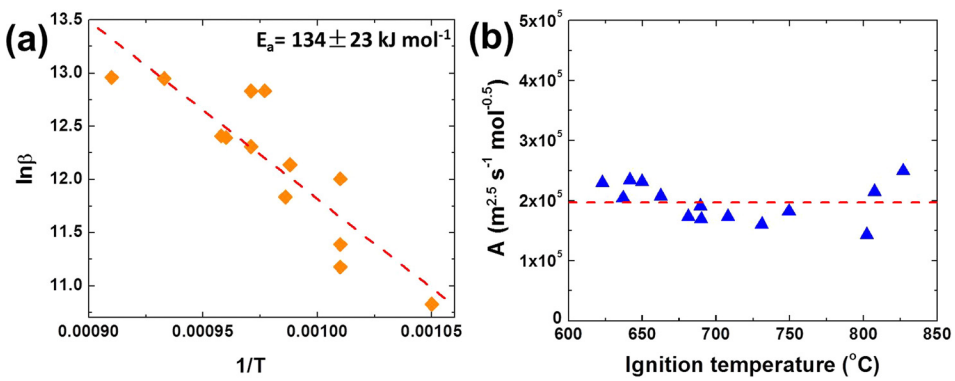

FIG. 5. (a) Arrhenius plot of heating rate vs ignition temperature at 1 atm O_2. The temperature unit here is Kelvin. (b) Relationship of the pre-exponential factor (A) with respect to the ignition temperature of n-Al under different O_2 pressures.

[This article is copyrighted as indicated in the article. Reuse of AIP content is subject to the terms at: http://scitation.aip.org/termsconditions. Downloaded to] IP: 128.8.176.93 On: Mon, 21 Sep 2015 14:12:05

further assume that the pre-exponential factors (A and A') are similar in Eqs. (10) and (14) ($= 2 \times 10^5$ $m^{2.5}mol^{-0.5}$ s^{-1}), then we can use these equations to better understand the differences between the four nanothermites (Fig. 2).

All $R_c's$ for the four thermite formulations were discussed before as the same constant ($\sim 5 \times 10^{-2}$ mol m^{-2} s^{-1}, see Table I). The concentration of Al can be estimated in a similar way as for n-Al, while the concentration of bound O can be estimated based on the oxygen densities of these oxidizers. Results show that both the concentrations of Al and bound O are close to constant for these four nanothermites. In terms of Eq. (14), the E_a^s values of condensed phase Al-O reaction for these thermite formulations can be obtained. In all cases, the thermites have larger activation energies than the direct reaction of n-Al with O_2 (Table I). This is not surprising since O_2 is freely available, which must be thermally released from the oxidizers. The other activation energies of condensed phase Al-O reaction follow: E_a^s (n-Al/Bi_2O_3) $< E_a^s$ (n-Al/K_2SO_4) $\approx E_a^s$ (n-Al/$K_2S_2O_8$) $< E_a^s$ (n-Al/Fe_2O_3). Since all R_c', A', C_{Al}^s, and C_O^s are constant for different nanothermites, the difference in activation energy is actually associated with the difference in ignition temperature for the four nanothermites in vacuum as: T (n-Al/Bi_2O_3) $< T$ (n-Al/K_2SO_4) $\approx T$ (n-Al/$K_2S_2O_8$) $< T$ (n-Al/Fe_2O_3) (Fig. 2).

(1) n-Al/Bi_2O_3 shows an invariant ignition temperature when O_2 pressure changes. This is because it has the lowest E_a^s among the four nanothermites, which is correlated to its high oxygen conductivity. Thus, even though this E_a^s is still larger than that for n-Al in O_2 (Table I), a two orders of magnitude higher C_O^s than that for O_2 determines that the ignition is dominated by condensed phased reaction; i.e., independent of O_2 pressure.
(2) For n-Al/$K_2S_2O_8$, the ignition temperature in vacuum is much higher, correlating to a higher E_a^s. However, it shows a similar constant ignition temperature as n-Al/Bi_2O_3 when the O_2 pressure is above 1 atm. In this case, the ignition mechanism is alternatively controlled by Al-O_2(g) reaction, and the reactant O_2 gas mostly from the decomposition of oxysalt which has a much higher oxygen concentration than that for the external O_2.
(3) For n-Al/K_2SO_4 and n-Al/Fe_2O_3, ignition is controlled by condensed phase reaction when O_2 pressure is <5 atm. The fact that n-Al/Fe_2O_3 shows a higher ignition temperature than n-Al/K_2SO_4 is consistent with the Arrhenius model that n-Al/Fe_2O_3 has a higher E_a^s. When O_2 pressure is >5 atm, their ignition temperatures approach that for n-Al in O_2. In this case, the effect of increased O_2 concentration favoring the Al-O(g) reaction becomes dominant.

The reader is reminded that the activation energies and reaction rates deduced in this work are presumably only valid for ignition and should not be assumed to be applicable to the whole combustion event.

IV. CONCLUSION

Ignition of n-Al and n-Al based energetic materials (nanothermites) was examined in different O_2 pressures aiming to differentiate the effects of free and bound oxygen. Results show that the ignition temperature of n-Al decreased as the O_2 pressure increased, whereas the ignition temperatures of nanothermites have different sensitivities to O_2 pressure depending on the formulations. We found that a constant critical reaction rate (5×10^{-2} mol m^{-2} s^{-1}) for ignition exists which is independent to ignition temperature, heating rate and free vs bound oxygen. The roles of oxygen concentration and activation energy of Al-O reaction were demonstrated based on the ignition results, and were reflected more quantitatively in a kinetic model. This study suggests that the ignition of n-Al based energetic materials is controlled by a constant R_c, and fit a simple Arrhenius model, leading to different ignition temperatures for different formulations.

ACKNOWLEDGMENTS

This work was supported by DOD/DTRA (BRBAA08-Per5-H-2-0065) and the Army Research Office. We also thank Dr. Greg Young of NSWC-IH for loan of his high pressure cell.

[1]C. Rossi, K. Zhang, D. Esteve, P. Alphonse, P. Tailhades, and C. Vahlas, J. Microelectromech. Syst. **16**, 919 (2007).
[2]R. A. Yetter, G. A. Risha, and S. F. Son, Proc. Combust. Inst. **32**, 1819 (2009).
[3]D. G. Piercey and T. M. Klapoetke, Cent. Eur. J. Energ. Mater. **7**, 115 (2010).
[4]E. L. Dreizin, Prog. Energy Combust. Sci. **35**, 141 (2009).
[5]N. H. Yen and L. Y. Wang, Propellants Explos. Pyrotech. **37**, 143 (2012).
[6]B. Siegert, M. Comet, and D. Spitzer, Nanoscale **3**, 3534 (2011).
[7]A. Vignes, F. Munoz, J. Bouillard, O. Dufaud, L. Perrin, A. Laurent, and D. Thomas, Process Saf. Environ. **90**, 304 (2012).
[8]E. M. Hunt and M. L. Pantoya, J. Appl. Phys. **98**, 034909 (2005).
[9]M. Schoenitz, B. Patel, O. Agboh, and E. L. Dreizin, Thermochim. Acta **507–508**, 115 (2010).
[10]J. Sun, M. L. Pantoya, and S. L. Simon, Thermochim. Acta **444**, 117 (2006).
[11]D. Spitzer, M. Comet, C. Baras, V. Pichot, and N. Piazzon, J. Phys. Chem. Solids **71**, 100 (2010).
[12]F. Severac, P. Alphonse, A. Esteve, A. Bancaud, and C. Rossi, Adv. Funct. Mater. **22**, 323 (2012).
[13]H. Wang, G. Jian, G. C. Egan, and M. R. Zachariah, Combust. Flame **161**, 2203 (2014).
[14]M. A. Trunov, M. Schoenitz, and E. L. Dreizin, Combust. Theory Modell. **10**, 603 (2006).
[15]D. A. Firmansyah, K. Sullivan, K-S. Lee, Y. H. Kim, R. Zahaf, M. R. Zachariah, and D. Lee, J. Phys. Chem. C **116**, 404 (2012).
[16]C. Snehaunshu, K. Sullivan, N. Piekiel, L. Zhou, and M. R. Zachariah, J. Phys. Chem. C **114**, 9191 (2010).
[17]L. P. H. Jeurgens, W. G. Sloof, F. D. Tichelaar, and E. J. Mittemeijer, J. Appl. Phys. **92**, 1649 (2002).
[18]A. Ermoline and E. L. Dreizin, Chem. Phys. Lett. **505**, 47 (2011).
[19]B. J. Henz, T. Hawa, and M. R. Zachariah, J. Appl. Phys. **107**, 024901 (2010).
[20]V. I. Levitas, B. W. Asay, S. F. Son, and M. L. Pantoya, J. Appl. Phys. **101**, 083524 (2007).
[21]S. Zhang and E. L. Dreizin, J. Phys. Chem. C **117**, 14025 (2013).
[22]A. Rai, K. Park, L. Zhou, and M. R. Zachariah, Combust. Theory Modell. **10**, 843 (2006).
[23]R. Nakamura, D. Tokozakura, H. Nakajima, J. G. Lee, and H. Mori, J. Appl. Phys. **101**, 074303 (2007).
[24]N. W. Piekiel, L. Zhou, K. T. Sullivan, S. Chowdhury, G. C. Egan, and M. R. Zachariah, Combust. Sci. Technol. **186**, 1209 (2014).
[25]L. Zhou, N. Piekiel, S. Chowdhury, and M. R. Zachariah, J. Phys. Chem. C **114**, 14269 (2010).
[26]G. Jian, J. Feng, R. J. Jacob, G. C. Egan, and M. R. Zachariah, Angew. Chem. Int. Ed. **52**, 9743 (2013).

[This article is copyrighted as indicated in the article. Reuse of AIP content is subject to the terms at: http://scitation.aip.org/termsconditions. Downloaded to] IP: 128.8.176.93 On: Mon, 21 Sep 2015 14:12:05

[27]W. Zhou, J. B. DeLisio, X. Li, L. Liu, and M. R. Zachariah, J. Mater. Chem. A **3**, 11838 (2015).
[28]W. Zhou, J. B. DeLisio, X. Wang, and M. R. Zachariah, "Reaction mechanisms of energetic composites containing potassium oxysalts as oxidizers," Combust. Flame (submitted).
[29]K. T. Sullivan, N. W. Piekiel, S. Chowdhury, S. T. Kelly, T. C. Hufnagel, K. Fezzaa, and M. R. Zachariah, Combust. Flame **159**, 2 (2012).
[30]R. J. Jacob, G. Jian, P. M. Guerieri, and M. R. Zachariah, Combust. Flame **162**, 258 (2015).
[31]K. T. Sullivan, W.-A. Chiou, R. Fiore, and M. R. Zachariah, Appl. Phys. Lett. **97**, 133104 (2010).
[32]G. C. Egan, K. T. Sullivan, T. LaGrange, B. W. Reed, and M. R. Zachariah, J. Appl. Phys. **115**, 084903 (2014).
[33]G. Jian, S. Chowdhury, K. Sullivan, and M. R. Zachariah, Combust. Flame **160**, 432 (2013).
[34]A. Rai, D. Lee, K. Park, and M. R. Zachariah, J. Phys. Chem. B **108**, 14793 (2004).
[35]J. Sivan, Y. Haas, D. Grinstein, S. Kochav, G. Yegudayev, and L. Kalontarov, Combust. Flame **162**, 516 (2015).
[36]M. A. Trunov, S. M. Umbrajkar, M. Schoenitz, J. T. Mang, and E. L. Dreizin, J. Phys. Chem. B **110**, 13094 (2006).
[37]K. Park, D. Lee, A. Rai, D. Mukherjee, and M. R. Zachariah, J. Phys. Chem. B **109**, 7290 (2005).
[38]M. Schoenitz, S. Umbrajkar, and E. L. Dreizin, J. Propul. Power **23**, 683 (2007).
[39]L. Zhou, A. Rai, N. Piekiel, X. Ma, and M. R. Zachariah, J. Phys. Chem. C **112**, 16209 (2008).
[40]S. Mohan, M. A. Trunov, and E. L. Dreizin, J. Heat Transfer **130**, 104505 (2008).
[41]T. S. Ward, M. A. Trunov, M. Schoenitz, and E. L. Dreizin, Int. J. Heat Mass Transfer **49**, 4943 (2006).
[42]M. A. Trunov, M. Schoenitz, and E. L. Dreizin, Propellants Explos. Pyrotech. **30**, 36 (2005).
[43]S. Alavi, J. W. Mintmire, and D. L. Thompson, J. Phys. Chem. B **109**, 209 (2005).
[44]C. Lanthony, J. M. Ducere, M. D. Rouhani, A. Hemeryck, A. Esteve, and C. Rossi, J. Chem. Phys. **137**, 094707 (2012).
[45]A. Ermoline, D. Yildiz, and E. L. Dreizin, Combust. Flame **160**, 2982 (2013).
[46]See supplementary material at http://dx.doi.org/10.1063/1.4930889 for (1) supplementary text on kinetic model of n-Al ignition; schematic of the wire heating experiments (Fig. S1); (2) schematic of energy and mass model at ignition (Fig. S2); (3) relationships between the aluminum/oxygen surface concentrations and the ignition temperature of n-Al under different O2 pressures (Fig. S3); (4) Arrhenius plot of heating rate vs. ignition temperature at 3 atm O_2 (Fig. S4); (5) relationships of ignition temperature and aluminum fluxes (Fig. S5); and (6) relationships between Al density/pressure gradient across the alumina shell, and the temperature (Fig. S6).
[47]W. Zhou, M. W. Orr, G. Jian, S. K. Watt, V. T. Lee, and M. R. Zachariah, Chem. Eng. J. **279**, 578 (2015).
[48]E. D. Wachsman, S. Boyapati, M. J. Kaufman, and N. Jiang, *Proceedings of the International Symposium Solid-state Ionic Devices* (Pennington, New Jersey, 1999), Vol. 1, p. 42.
[49]See http://webbook.nist.gov/cgi/cbook.cgi?ID=C7429905&Units=SI&Mask=2#Thermo-Condensed for the heat capacity of Al.
[50]N. Cabrera and N. F. Mott, Rep. Prog. Phys. **12**, 163 (1949).
[51]G. Jian, N. W. Piekiel, and M. R. Zachariah, J. Phys. Chem. C **116**, 26881 (2012).
[52]H. Flynn and L. A. Wall, J. Res. Natl. Bur. Stand. **70A**, 487 (1966).
[53]T. Ozawa, Thermochim. Acta **203**, 159 (1992).
[54]G. Jian, L. Zhou, N. W. Piekiel, and M. R. Zachariah, ChemPhysChem **15**, 1666 (2014).

[This article is copyrighted as indicated in the article. Reuse of AIP content is subject to the terms at: http://scitation.aip.org/termsconditions. Downloaded to] IP: 128.8.176.93 On: Mon, 21 Sep 2015 14:12:05